
Article:
Farrimond, D.G. orcid.org/0000-0002-9440-4369, Woolford, S., Barr, A.D. et al. (10 more authors) (2024) Experimental studies of confined detonations of plasticized high explosives in inert and reactive atmospheres. Proceedings of the Royal Society A: Mathematical, Physical and Engineering Sciences, 480 (2294). ISSN 1364-5021

https://doi.org/10.1098/rspa.2024.0061

PROCEEDINGS A

royalsocietypublishing.org/journal/rspa

Research

Cite this article: Farrimond DG *et al*. 2024 Experimental studies of confined detonations of plasticized high explosives in inert and reactive atmospheres. *Proc. R. Soc. A* **480**: 20240061.
https://doi.org/10.1098/rspa.2024.0061

Received: 5 February 2024
Accepted: 10 June 2024

Subject Category:
Engineering

Subject Areas:
civil engineering, structural engineering, chemical engineering

Keywords:
blast parameter variability, confined blasts, quasi-static pressure, afterburn, numerical modelling

Author for correspondence:
D. G. Farrimond
e-mail: d.farrimond@sheffield.ac.uk

Electronic supplementary material is available online at https://doi.org/10.6084/m9.figshare.c.7351601.

THE ROYAL SOCIETY PUBLISHING

Experimental studies of confined detonations of plasticized high explosives in inert and reactive atmospheres

D. G. Farrimond[1,2], S. Woolford[1,2], A. D. Barr[1], T. Lodge[1,2], A. Tyas[1,2], R. Waddoups[1,2], S. D. Clarke[1,2], S. E. Rigby[1,3], M. J. Hobbs[4], J. R. Willmott[4], M. Whittaker[5], D. J. Pope[5] and M. Handy[6]

[1]Department of Civil & Structural Engineering, University of Sheffield, Sheffield S1 3JD, UK
[2]Blastech Ltd. The Innovation Centre, 217 Protobello, Sheffield S1 4DP, UK
[3]Arup Resilience Security & Risk, 3 Piccadilly Place, Manchester M1 3BN, UK
[4]Department of Electronic & Electrical Engineering, University of Sheffield, Sheffield S1 4DT, UK
[5]Defence Science and Technology Laboratory, Salisbury, UK
[6]Kent PLC. 1 Lochrin Square, 92-98 Fountainbridge, Edinburgh EH3 9QA, UK

DGF, 0000-0002-9440-4369; RW, 0000-0002-2241-3784; SDC, 0000-0003-0305-0903

When explosives detonate in a confined space, repeated boundary reflections result in complex shock interactions and the formation of a uniform quasi-static pressure (QSP). For fuel-rich explosives, mixing of partially oxidized detonation products with an oxygen-rich atmosphere results in a further energy release through rapid secondary combustion or 'afterburn'. While empirical formulae and thermochemical modelling approaches have been developed to predict QSP, a lack of high-fidelity experimental data means questions remain around the deterministic quality of confined explosions, and the magnitude and mechanisms of afterburn reactions. This article presents experimental data for RDX- and PETN-based plastic explosives, demonstrating the high repeatability of the QSP generated in a sealed chamber using pressure transducers and high-speed infrared thermometry. Detonations in air, nitrogen and argon atmospheres

are used to identify the contribution of afterburn to total QSP, to estimate the duration of afterburn reactions and to speculate on the flame temperature associated with this mechanism. Computational fluid dynamic modelling of the experiments was also able to accurately predict these effects. Understanding and quantifying explosions in complex environments are critical for the design of effective protective structures: the mechanisms described here provide a significant step towards the development of fast-running engineering models for internal blast events.

1. Introduction

Upon explosive detonation, a hot, dense fireball, often containing only partially oxidized constituents, is released. The expansion of the fireball cloud generates shock waves in the surrounding atmosphere, which propagate away from the location of the detonation. In confined explosions, multiple reflections of the resulting shock waves will violently mix the detonation products with the chamber atmosphere. If oxygen is present in this atmosphere, the fireball contains non-fully oxidized constituents, and the temperature remains high enough that a secondary combustion or 'afterburn' may occur. This releases additional thermal energy when the fireball comes into contact with surrounding oxygen [1]. Kuhl *et al*. [2] undertook a numerical simulation to discover that the aforementioned combustion rate is dependent on the chamber size, which logically can be directly related to the time in which forced mixing occurs from the interactions of reflected shocks and the fireball.

These shock wave interactions are complex, but over time, the individual shocks decay and, in the absence of thermal energy losses or venting, a uniform quasi-static pressure (QSP) above the ambient value will exist in the space. The magnitude of the QSP is governed by the volume of the space, the volume of gas generated by the explosion and the energy released. These parameters result in increases in the internal temperature and thus the pressure. The situation is made more complex by the fact that most high explosives are fuel rich. This means that an 'afterburn' reaction can result in an additional energy release when mixing occurs with the surrounding medium. This additional energy release is a direct result of the full detonation and deflagration of the explosive and its products, respectively [3]. Wolanski *et al*. [4] verified these findings when visualizing the performance of small chamber detonations of gram-scale TNT in different environments. The resulting high-speed imagery exhibited more pronounced instability structures within an oxygen-rich medium at the same time after detonation in nitrogen or argon atmosphere.

The simplest type of prediction of QSP magnitudes comes from empirical predictive formulae, derived from experimental observations of confined TNT detonations. Using dimensional analysis techniques showed that the peak QSP was a function of the ratio of charge mass to chamber volume, while (ignoring thermal energy loss) the decay of the QSP was a function of the peak QSP and the vent area-to-chamber volume ratio. This resulted in a predictive formula derived from the analysis of a large amount of experimental data [5]. Here, the charge mass may be thought of as a surrogate for the gas and energy release owing to the explosion.

At the other extreme, QSP can be estimated by a detailed numerical model of a detonation and subsequent propagation of the air shocks and mixing of the detonation products [6]. The accuracy of these approaches varies depending on the way in which energy release is modelled owing to the afterburn reactions and is typically computationally expensive. Donahue *et al*. [7] were able to develop new equations of state, which although 9% longer in run time than standard numerical methods, resulted in an excellent transient and quasi-static agreement to experimental data.

A third approach is to perform a simplified thermochemical analysis aimed at predicting both the release of energy and the overall effect on the QSP. Codes such as CHEETAH [8,9] perform detailed calculations of the chemical reactions at various thermal states and can be used to predict the resulting gas mixture, temperature and pressure within a confined space [10]. However, these codes are not always available to the general user, and the level of detail may not always be appropriate to real-world conditions where the threat may not be well defined.

Lacking is a distinct experimental benchmark of confined QSP resulting from explosive detonation in different atmospheres, offering insight into the question of whether the results are deterministic and repeatable. This article describes such an experimental study of small-scale, fuel-rich RDX- (PE4 and PE8) and PETN-based (PE10) plasticized high explosives. The resulting pressure–time traces are demonstrated to be highly consistent over several repeat tests. Afterburn features are identified and the duration and effects on peak QSP values quantified. High-speed measurements of the post-detonation temperature are shown that may indicate the flame temperature of the afterburn reactions. Finally, we will demonstrate that ideal gas conditions apply, by independently measuring pressure and temperature in a confined explosion and showing that they satisfy the ideal gas equation and hence supporting the predictive approach proposed by Edri *et al*. [11,12].

2. Review of literature

Explosions that occur within a partially or fully confined space are far more detrimental than similar-sized explosives within a free-air environment [13]. This is directly related to the geometrical parameters within which the event occurred that is charge location, geometry of environment and the presence of openings. The complexity of confined explosions is mainly due to three distinct mechanisms [14,15]. The first mechanism is directly related to the initial propagation of a high-pressure shock wave, which has been reported on in many published articles and defined with high consistency [16,17]. When within a confined space, these interact with boundaries and reflect back towards the explosive centre resulting in complex turbulent interactions within the detonation cloud and further combustion energy release [18]—the second mechanism. The last mechanism being the pressure losses within the system as the pressure–time history profile begins to decay over a longer duration of time. Feldgun *et al*. [19] undertook both experimental and numerical simulations of confined explosive temporal behaviours wherein the decay mechanism magnitude and form exhibited a direct relationship with the chamber volume. This led to the conclusion of this decay being related to a thermal loss when raising the temperature of the boundary material.

Weibull [20] conducted a regime of confined trials with a variety of chamber geometries and volumes. The overall aim was to characterize the temporal QSP behaviour of a given explosive with respect to a mass-to-chamber volume ratio. The empirical dataset was collected on a speculative basis with limited theoretical justification, but despite this showed a clear and significant relationship between the maximum QSP and volume ratio. This was a fundamental outcome and development in the prediction of confined overpressure that was used to develop the predictive curves within UFC 3-340-02 [21].

Edri *et al*. [18] conducted confined experimental trials using varying masses of TNT to analyse the resulting gas pressures and compared them directly with UFC 3-340-02 [21]. The aim was to further quantify the effects of charge mass within a given confined space and present similar linearity in the findings to that of Weibull [20]. The aforementioned design manual, however, over-predicted the QSP by 27%, which was attributed to the methodology of analysis.

The works of Feldgun *et al*. [19] and Edri *et al*. [11] have proposed a number of semi-empirical/analytical methods for the prediction of internal gas pressures. These were derived from

explosive detonation being based on the conservation of energy and ideal gas theory. Both include afterburn or combustion of the binder material of an explosive, which shows considerable agreement with the limited experimental data available.

Kuhl *et al*. [1] undertook testing regimes of TNT within different atmospheres to highlight the effect of afterburn. This provided a baseline for all confined explosive measurements and began the discussion around afterburn as a phenomenon but lacked the fidelity to determine time scales that it acted over.

Efforts have been made at capturing the behaviour of confined blasts using numerical modelling [12] with the inclusion of afterburn. Provided the parameters are iteratively solved to match experimental data, there is significant agreement. These empirical factors, however, have been related directly to the wave speeds within the complex fireball where the lack of fundamental understanding causes difficulty in theoretical assignment [22].

Edri *et al*. [12] detailed a methodology of predicting QSP based on the atmospheric pressure of the system and the detonation energy released during the event. Based on the theoretical analysis contained within this aforementioned article, it was determined that 3.17 kg air/kg TNT is required for a maximum energy release through combustion afterburn. Naturally, this value will be different for other explosives, as it is dependent on the amount of unreacted 'fuel' (predominantly partially oxidized or unoxidized carbon) following the initial detonation reaction. If more air is available within the system (i.e. smaller reduced mass ratio), full combustion will occur with less air, the system would be oxygen deficient and therefore the reaction will terminate at a lower overall energy release, resulting in lower temperature and pressure in the confined atmosphere.

Data from 11 historical references (table 1) investigated confined gas pressures from TNT detonations, within a variety of chamber volumes, which are displayed in figure 1. The two inclined straight trendlines demonstrate the QSP magnitude predictions for different TNT-reduced mass, derived from the ideal gas energy equation (2.1):

$$P = (\gamma - 1)/V, \tag{2.1}$$

where P is the absolute pressure, γ is the (temperature and gas formulation dependent) ratio of specific heat capacities and V is the confined volume. The upper line is the pressure that would be predicted assuming full release of all the explosive's reaction energy (i.e. an oxygen-rich chamber atmosphere, with all detonation products fully oxidized) while the lower line represents the prediction when only the detonation reaction occurs, with no subsequent afterburn (i.e. an oxygen-free chamber atmosphere). The cranked line is the prediction presented in UFC 3-340-02 [21], derived from experimental studies by Weibull [20].

While the predictions broadly match the experimental data, there is considerable spread, considering the log–log axes. This leaves unanswered the questions of whether this is an inherent variability, or owing to experimental error, and how accurately we might be able to predict the results from a well-controlled experimental trial.

3. Experimental methodology

The testing regime documented within this article consisted of 42 confined blast tests using PE4, PE8 and PE10 explosives, charges across a range of masses between 10 and 50 g. Tests were carried out inside of a 592 mm internal diameter, 1002 mm long cylindrical steel tube with a volume of 275.8 ± 2 l, which was confined by fixing two 50 mm thick steel end plates to either end of the pipe with a rubber gasket between the chamber and plate inducing a gas tight seal. Details of the blast chamber are presented within figure 2. As part of this testing regime, the effect of chamber atmospheres on explosive yield was assessed through filling the chamber with a variety of different gases. These plasticized explosives are based on RDX (PE4 and PE8) or PETN (PE10), which have oxygen balances of −21.6 and −10.1%, respectively. The additional

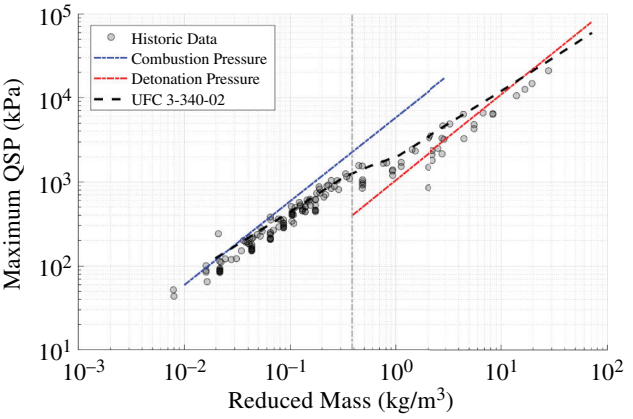

Figure 1. Compiled QSP data from TNT detonations of varying mass, chamber volume and shape from 11 external references with reference to predicted energy releases presented by Edri *et al*. [12].

Table 1. References of confined gas pressures as a result of TNT detonations.

Reference	Mass (kg)	Volume (m^3)
Maiz & Paszula [23]	0.043	0.15
Weibull [20]	0.01–125	0.410–28.2
Feldgun *et al*. [19]	1.7–2.1	32.5
Zhang *et al*. [24]	1–4	26
Zhou *et al*. [25]	0.040–0.250	1.152
Esparza *et al*. [26]	N/A	N/A
Edri *et al*. [18]	0.5–4	23.1
Kong *et al*. [27]	0.015–0.200	0.144–1.152
Carney *et al*. [28]	0.014–0.02	0.00687
Willauer *et al*. [29]	4–23	182.3
Chen & Xu [30]	0.005–0.03	0.00179
Kinney *et al*. [31]	N/A	N/A

fuel provided by the binder materials significantly increases their overall oxygen deficiency: typical ratios of explosive and binder indicate approximate oxygen balances of −84% for PE4, −78% for PE8 and −69% for PE10.

To enable a fully sealed pipe, a removable plug mechanism was developed for an effective charge placement externally of the chamber which could then be affixed to the pipe. A rubber gasket was placed between the plug's face and the external face of the chamber once the charge and detonator were in position, providing a fully confined seal. The explosive charge was set on a cradle, designed to be essentially non-invasive to the expansion of the detonation products and of limited chemical reactivity, while allowing accurate placement of the charge.

Connected to the plug's internal face were two 4 mm diameter steel supporting rods, set 75 mm apart. A lightweight fibreglass mesh sheet (total mass <0.5 g) spanned between the rods, centred 240 mm from the end plate internal wall and along the chamber axis, providing a stable base for the charge.

Charges were detonated using a Euronel non-electric detonator (0.8 g TNT equivalent mass of explosive). The detonator shock tube was fed through a 2 mm hole in the removable plug, so

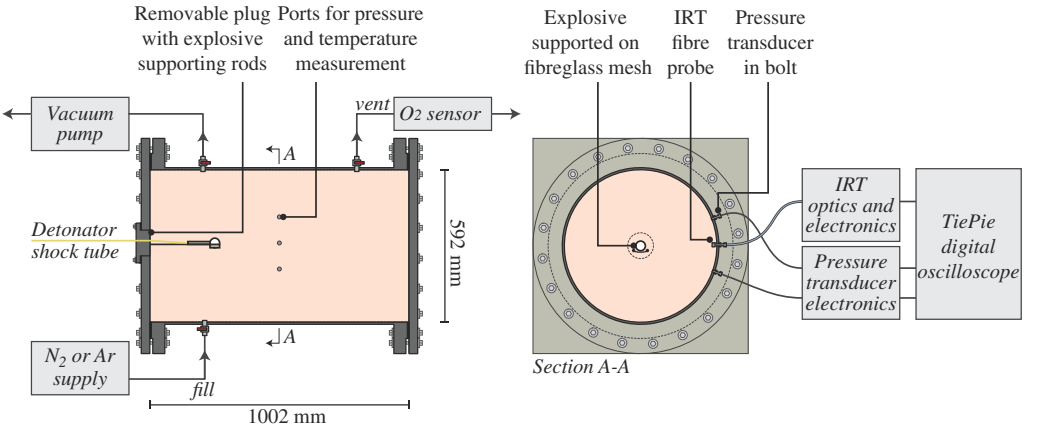

Figure 2. Confined blast chamber schematic detailing positions of pressure gauges and infrared radiation thermometers.

the charge and detonator could be positioned before inserting the plug into the chamber. This hole was machined such that the shock tube fitted tightly within it, to reduce any detonation products venting from the chamber during each test.

During the baseline development trials, the explosives were detonated in the ambient air internal to the chamber. Variation of the chamber gases required a procedure to be developed to ensure a negligible volume of ambient air remained in the chamber pre-test. To do so, taps allowed for both purging of the ambient chamber atmosphere, using a vacuum pump and fully sealing the chamber. Once the chamber was fully sealed with charge in place, a gas of choice was pumped into the chamber. This was done to ensure adequate mixing of the gases occurred in the pipe in the attempt to avoid pockets of ambient air prior to testing. On the exit valve of the chamber, a greisinger GOX100 oxygen meter was attached to the pipeline, measuring the purged gas oxygen percentage exiting the chamber. For all tests with different tested atmospheres, the gas was continually purged until a value of 0.2% oxygen was recorded and was stable on the sensor for over 5 min. After each test was conducted, the debris and residue were cleared from the pipe to ensure a consistent testing apparatus across the whole regime of trials.

The pressure–time history of each trial was recorded using a 17 bar Kulite HKM-375 and a 35 bar HEM-375M piezo-resistive pressure gauge, capturing the early-time shock propagation of an explosive event alongside the late-time build-up of internal QSP. Two pressure gauges of different ratings were used to establish data reliability across a single test. The two pressure gauges were located in the centre of the pipe, approximately 50 cm from each end, positioned along the circumference of the chamber as per figure 2. Prior to any test, pressure gauges were tested against known static pressures to confirm the gauge calibration factor. The pressure–time histories were recorded using a 16-bit digital oscilloscope and TiePie software, with a sampling rate of between 48 and 78 kHz (13–21 ms per sample) at 16-bit resolution.

(a) Thermal stability and protection of pressure gauges

The pressure gauges are prone to damage from fragment impact and long-term exposure to high temperature. In a confined detonation, high-speed fragments from the detonator casing may be generated, and the fireball may reach temperatures in excess of 5000K. Consequently, it was decided to insulate the gauges from these risks.

The system developed for this testing regime consisted of a 70 mm long M16 bolt with a cored 10 mm diameter hole 35 mm along from one end of the bolt, acting as the air reservoir allowing a realistic measurement of atmospheric pressure. At the other end of the bolt, a 3 mm diameter hole was cored through the bolt to meet the reservoir, providing a narrow passage for

pressurized gases to enter the reservoir and interact with the gauges. The bolt was mounted to the chamber creating an airtight seal, to maintain the fully confined nature of the tests (figure 3).

This approach inevitably means that the pressure gauges would not accurately record the characteristics of at least the first shock reaching the chamber wall since the length of the air reservoir in the insulating bolt would act to attenuate the magnitude of the shock wave reaching the pressure gauge itself, relative to the parameters of the wave reaching the chamber wall, by essentially acting as a localized partial vent. Since the primary interest of this study was the longer term pressure development, this was considered a reasonable penalty to accept. Tests were conducted to ascertain whether the insulating bolt mounting affected the longer term measurements by mounting a gauge directly in the chamber wall adjacent to the insulating bolt.

An example of the resulting pressure traces is presented in figure 4. Clearly, the long-term internal pressure build measured within the pipe is comparable for both gauges, providing reassurance to the overall effectiveness of pressure recording when the gauge is mounted out of the direct line of the fireball. Other than the attenuation of the first shock, the two traces are broadly similar over both the short and very long term.

4. Experimental results

(a) Confined trial raw data consistency and processing

One of the main objectives of this research was to establish the consistency of nominally identical trials. A discussion continues in the blast characterization community on the expected variability of pressure waves generated by unconfined high explosive detonations. Farrimond *et al*. [17] present a detailed argument that, given careful control over the test conditions, the expected variability in recorded unconfined blast wave parameters should typically be no more than a few per cent of the mean in far-field scaled regimes (> 3 m/kg $^{1/3}$). A key aim of this study was to assess whether this level of consistency could be observed in the far more complex case of a confined detonation.

Figure 5 displays raw pressure–time histories from four nominally identical detonations of a 50 g sphere of PE4 in an air atmosphere, where each progressive plot displays a reduced time scale. When considering the earliest stage of the event, 0–5 ms, the raw individual shocks recorded are almost identical in magnitude, duration and arrival. This provides confidence in the consistency of the early-stage development of the fireball and the subsequent propagation of shock waves through the chamber. From 5 ms onwards, although the overall average pressure–time histories are very consistent between tests, the individual shocks begin to become slightly less aligned, perhaps indicating local variations in mixing of the detonation products and the chamber atmospheres, resulting in differences in shock velocity. However, as the longer term graph shows, as the shocks decay with time and the conditions within the chamber tend towards spatial uniformity, the QSP magnitude is very similar across all four tests. The data in figure 5 clearly and unequivocally demonstrate that test-to-test consistency is to be expected in confined explosions of plasticized high explosives.

Overlaid on each of these graphs is a Time-Dependent Smoothed Average (TDSA) for the remainder of this article, which is a commonly used method for determining the maximum QSP within a confined pipe [1]. The proposed TDSA method was coded into MATLAB, which automated the fitting process to the raw data. The method varies the number of data points used to find an average depending on the variation in the overall recorded pressure data; for parts of the recording that exhibit large changes in pressure, such as the arrival of the first shock wave at the gauge, the method will adopt a small sampling range, whereas in parts of the recording where the change in overall pressure is minimal, the sampling range increases. The adopted method provides an adequate fitting technique to the raw data in which

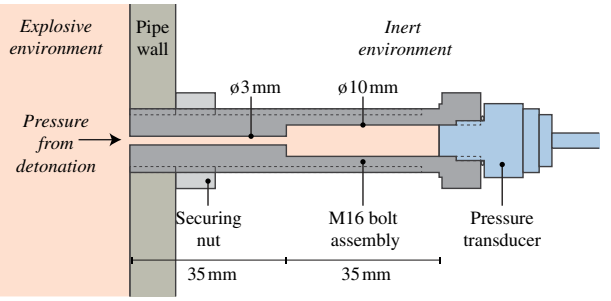

Figure 3. Schematic detailing the thermal isolation mechanism adopted to protect instrumentation during confined trials.

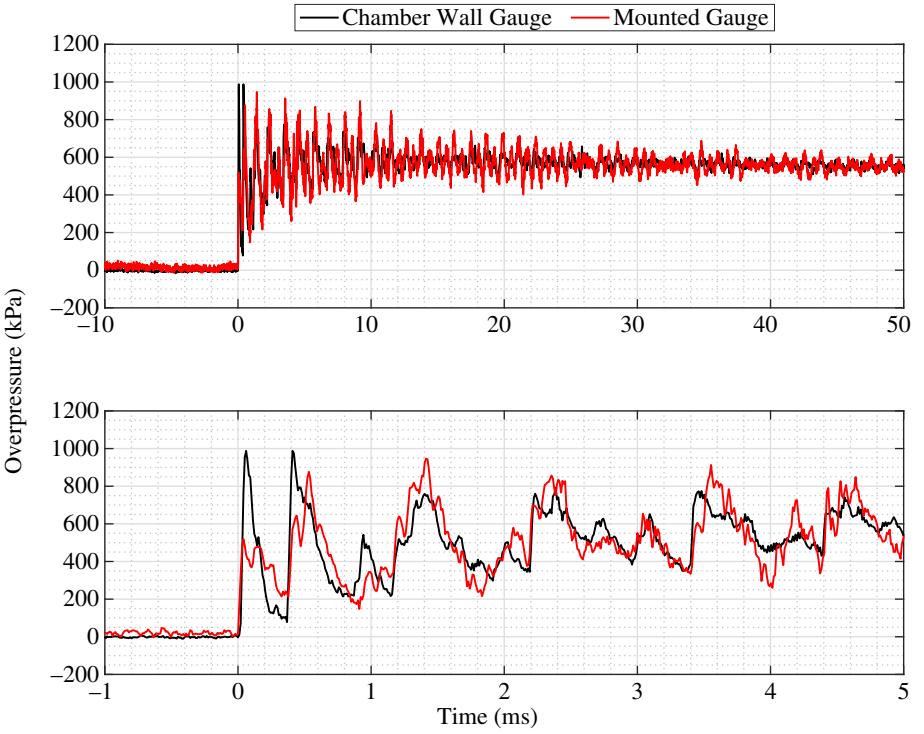

Figure 4. Raw pressure–time history plot for 50 g sphere of PE4 detonated within an air atmosphere with a pressure gauge taking measurements from direct line of sight to the fireball, installed on the chamber wall, and a gauge mounted in the protective bolt assembly.

a maximum QSP value can be determined and will be used to establish the parameter for all trials conducted as part of this research.

The decay in QSP seen in figure 5 over long time scales is believed to be due to thermal losses from the hot confined atmosphere to the cooler steel walls of the chamber. This phenomenon is being investigated within the wider research project but is not considered further within the context of this article due to it only becoming a prominent feature much after the maximum QSP is achieved.

Figure 6 displays three similar plots to the previous, displaying different considered time scales. When considering the maximum QSP from a given trial, the complexity of the shock interactions and chaotic mixing of hot gases results in difficulty when prescribing the exact magnitude of the peak. Highlighted is the ability of the TDSA method to capture the general

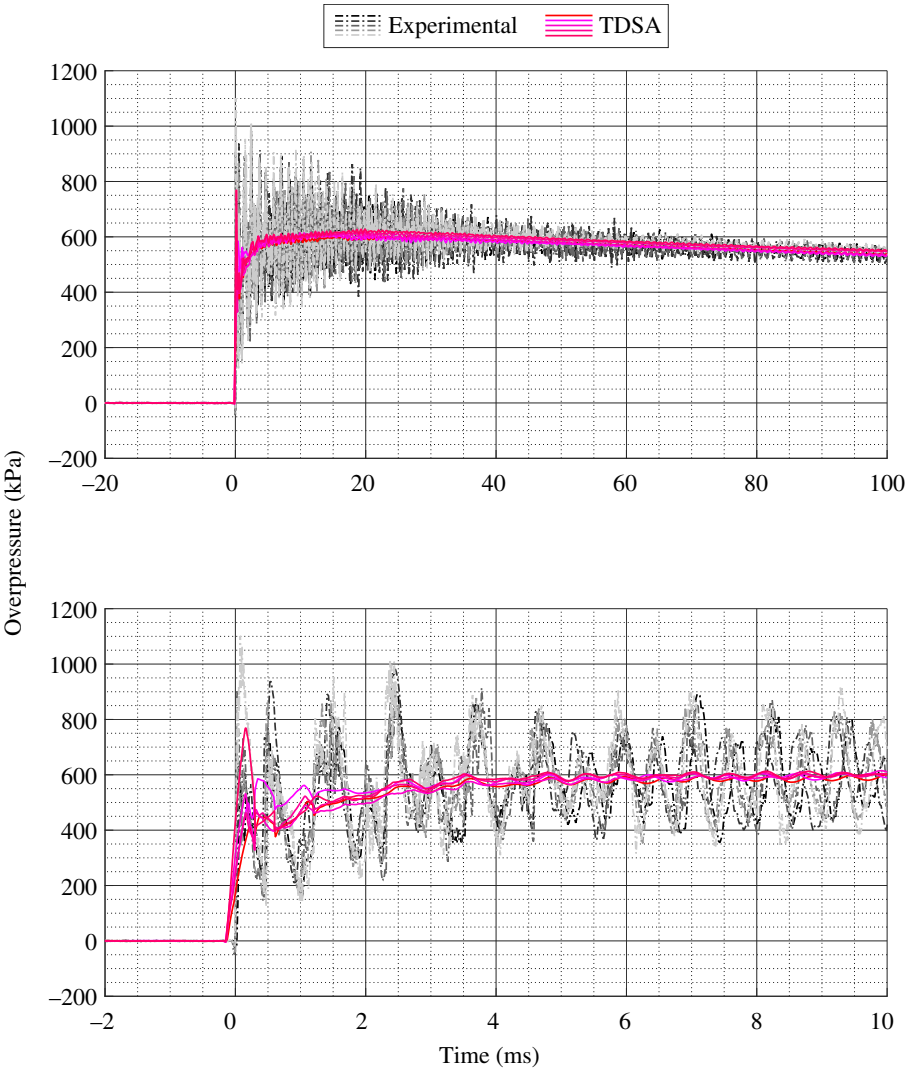

Figure 5. Raw pressure–time history plots from five nominally identical 50 g PE4 spherical detonations within the described confined chamber, within an air atmosphere across two different time scales of interest.

behaviour of a confined explosion without taking into account the complexity of each shock interaction within the vessel.

(b) Effect of charge shape

A preliminary study within this test series was to assess the effect of charge shape on the overall QSP within a confined chamber, and in order to do so, two tests using 50 g of PE4 moulded into a sphere and 2 : 1 cylinder were detonated within air. The charges used within these initial trials were formed using a three-dimensional-printed mould to ensure that the charges were as accurate to the desired shape as possible, removing any element of variability associated with this.

The data presented in figure 7 display the development of pressure with respect to time within the confined chamber for both spherical and cylindrical charges. The raw results emphasize that the individual shock waves exhibit slight differences in magnitude and arrival within the time scale presented. Interesting to note is that the cylindrical charges in the opening

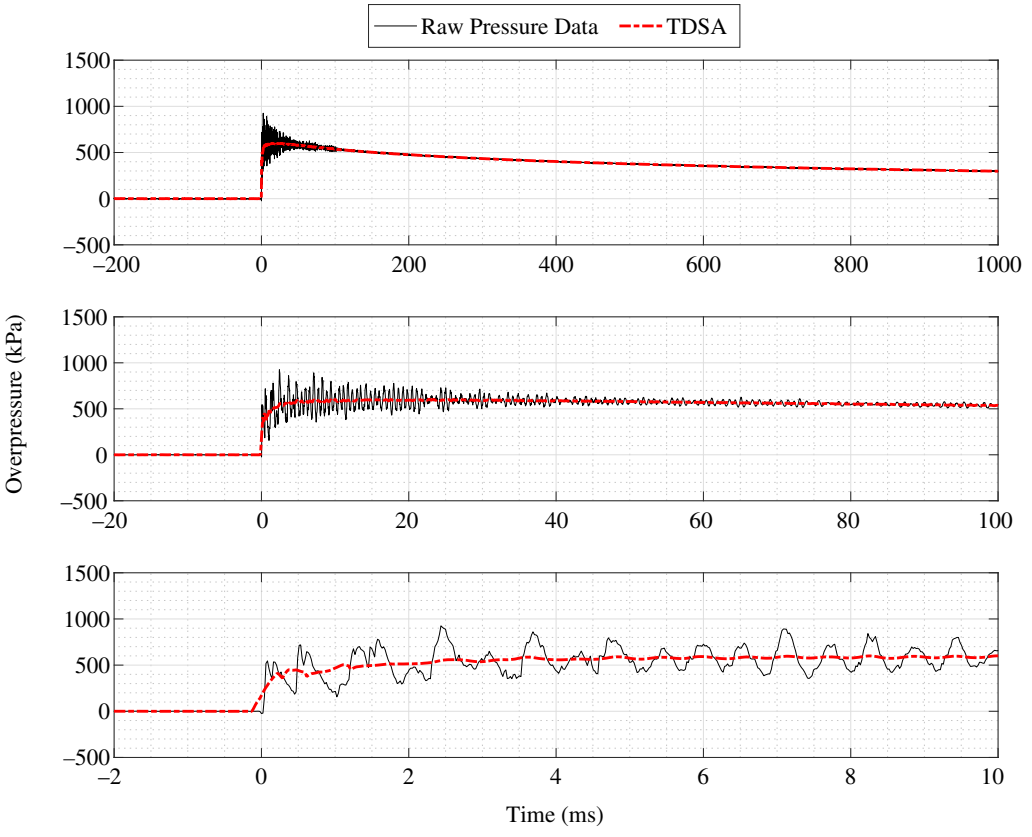

Figure 6. Raw pressure–time history plots for 50 g PE4 spherical detonations within the described confined chamber, within an air atmosphere across three different time scales of interest, with the evaluated TDSA overlain.

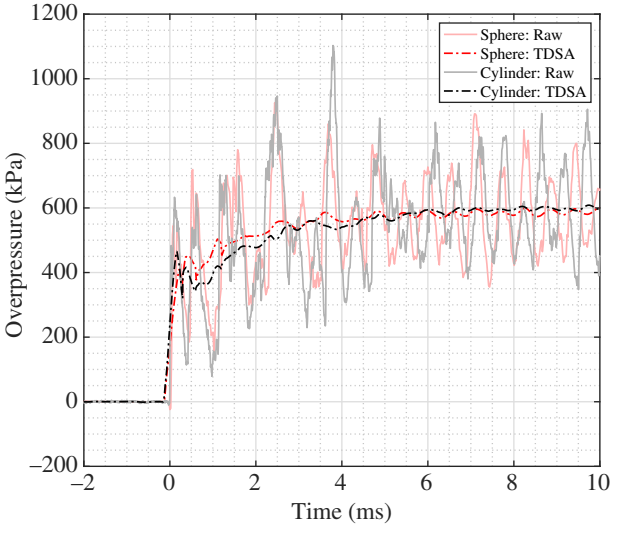

Figure 7. Raw pressure–time history plots for both 50 g sphere and cylinder PE4 detonations within the described confined chamber, denoted by red and blue lines are the TDSA for each test evaluating a peak QSP.

of few shocks (<2 ms) result in much lower magnitudes when compared with a spherical blast, which is directly linked to the directionality of the shock wave/fireball propagation in the early stages of breakout [32].

As the pressure gauges are located centrally along the pipe around its circumference, it is assumed that the initial longitudinal breakout of cylindrical charges results in a much lower proportion of the energy being captured on the gauges at this stage. Later in the recording (2–6 ms), the larger peaks associated with the cylindrical charge have been associated with the collision and chaotic mixing of the longitudinal shock waves in the pipe centre, resulting in a doubling of the pressures. This phenomenon was documented in free-field trials looking at the collision of multiple shock waves [33].

After 5 ms, the raw data for both trials tend to behave similarly as a result of the overall shock wave propagation in the system coalescing into a complicated shock structure. Prior to this, the pseudo-radial expansion of detonation products, resulting from changes in the original charge mass, and their interaction with the surrounding air atmosphere, results in variations in the rate at which combustion occurs. By 10 ms, the QSP recorded is consistently suggesting full detonation and combustion has occurred.

Overlaid on the raw pressure traces is the TDSA for each shot that have been evaluated using the aforementioned method in this article. It is evident to see that, despite the raw individual peaks varying in magnitude and arrival time when comparing the two charge shapes, the overall max. QSP is in essence the same. This finding was a fundamental discovery for confined blast loading in that the peak QSP is not charge shape dependent and therefore spheres could be considered for the remainder of this article. This finding is in line with hypotheses set out by Taylor [34], which suggests explosives can be defined by a point release of energy. In a confined environment, this means the internal pressure and temperature are a function of mass and energy released during detonation and deflagration of a given composition.

(c) Effect of the chamber atmosphere

The results presented in figure 8 represent two similar tests using a 50 g sphere of PE4 detonated within ambient air and nitrogen atmospheres. The main aim of these tests was to establish a fundamental understanding of the afterburn phenomenon, the physical mechanisms required for it to occur and under what time scales. Nitrogen was chosen as an alternative to ambient air due to exhibiting a similar density but devoid of oxygen and therefore eliminating any combustion effects resulting from the surrounding medium. Detonations in air and nitrogen, upon the first shock interacting with the pressure gauge, are almost identical in terms of shock magnitude; however, the impulse of the air shot is seemingly higher. Balakrishnan *et al*. [35] compared both a one- and three-dimensional approach for modelling a free-air TNT detonation in an attempt to establish the mechanisms of afterburn in an open environment. The article showed that when three-dimensional turbulent mixing is enabled, a clear increase in the overall impulse of the shock loading occurs and the secondary shock wave arrives sooner in comparison with a one-dimensional model. This finding is similar to what is shown in figure 8 in that when oxygen is present, afterburn (or better termed 'combustion') begins the moment the fireball comes into contact with the surrounding medium.

Interestingly, upon the arrival of the second shock recorded, the magnitude of the pressure recording in air is almost double that of the nitrogen atmosphere. The nitrogen atmosphere prevents secondary oxidation of the fuel-rich detonation cloud so effectively prevents the afterburn reaction. The differences in pressure–time between the two atmospheres are directly related to the forced mixing of detonation products with the surrounding atmosphere.

An alternative inert atmosphere was investigated by filling the chamber with argon. Zhang *et al*. [36] explained that despite argon having one of the best inerting abilities of all the noble gases, there are limited data reporting on its use for fuel-related processes or combustion

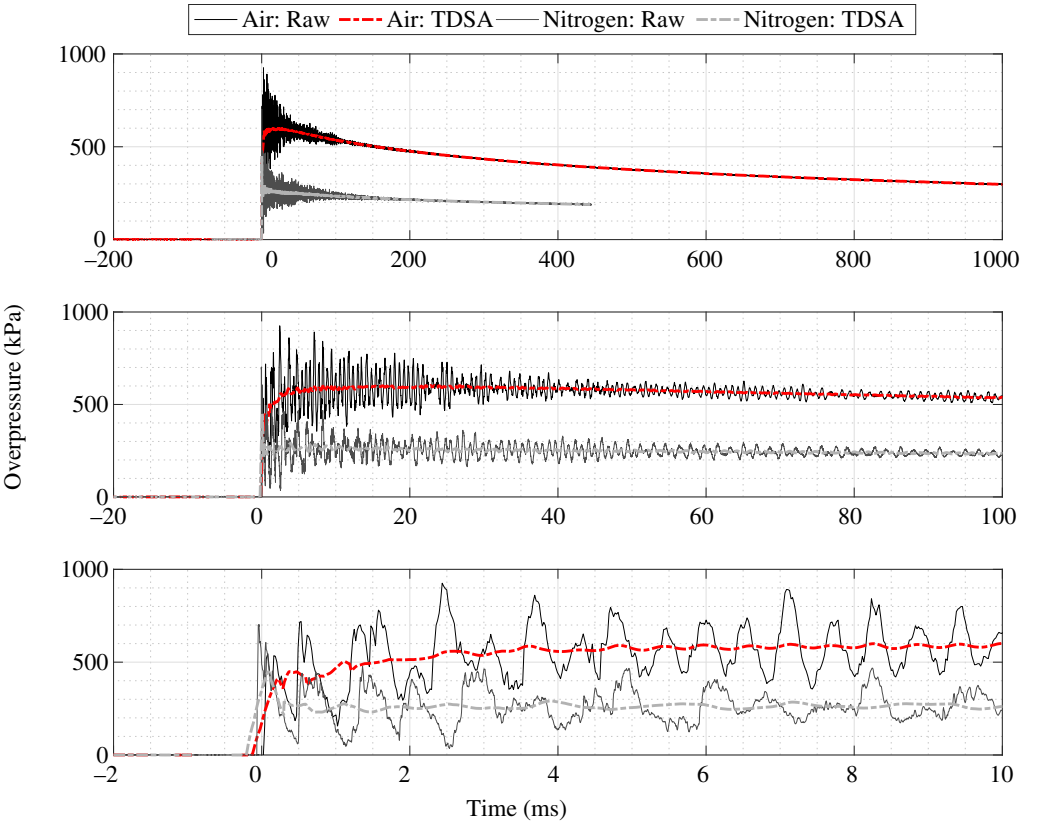

Figure 8. Raw pressure–time history plots for 50 g PE4 spherical detonations within the described confined chamber, with air and nitrogen atmospheres.

during explosive events. Argon having different physical properties, such as density and heat capacity, in theory would result in a different QSP than in a nitrogen atmosphere, despite the explosive exhibiting the same detonation energy. Trzcinski *et al*. [37] investigated the behaviour of explosives with non-ideal characteristics in air, nitrogen and argon atmospheres and confirmed that while combustion did not occur in argon, a greater pressure was experienced than in nitrogen. The results presented in figures 9 and 10 validate these findings.

The first recorded shocks are almost identical across all three atmospheres while the subsequent shocks begin to vary in phase and magnitude. As mentioned earlier, the immediate interaction with the surrounding atmosphere results in the later deviations in individual shock behaviours and the overall QSP. The second shock within the air atmosphere arrives sooner alongside having a greater magnitude and duration, when compared with nitrogen and argon. This indicates that the afterburn mechanism begins upon the interaction between the detonation products, immediately behind the incident shock, and the surrounding atmosphere. This finding is in line with the work of Kuhl *et al*. [1] and supports the suggestion of Balakrishnan *et al*. [35] that afterburn of a hot, fuel-rich detonation cloud will become significant as soon as there is any mechanism to provoke a mixing of the cloud with a surrounding atmosphere containing oxygen. Figure 11 represents the physical mechanism of afterburn by which an additional energy release occurs through the mixing of the surrounding oxygen with the fireball.

The comparison between the inert atmospheres, however, is not evident from the first shock wave. As the explosives detonate with the same energy release, the resulting shock waves travel effectively identically. The difference seen between these trials is that within the argon

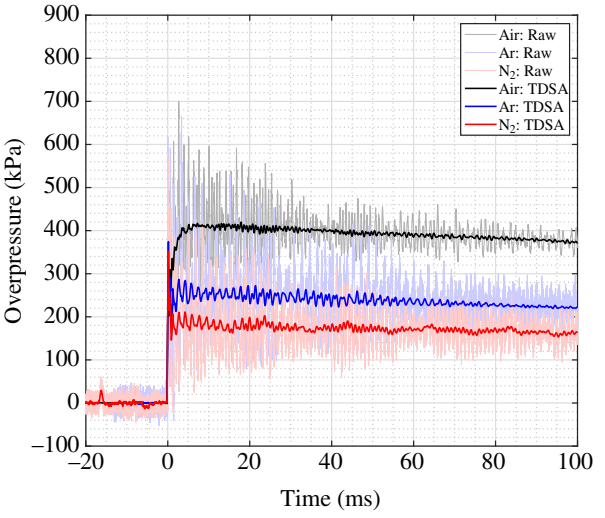

Figure 9. Raw pressure–time history plots for 30 g PE10 spherical detonations within the described confined chamber, with air, nitrogen and argon atmospheres, with the TDSA fit of each test plotted for reference.

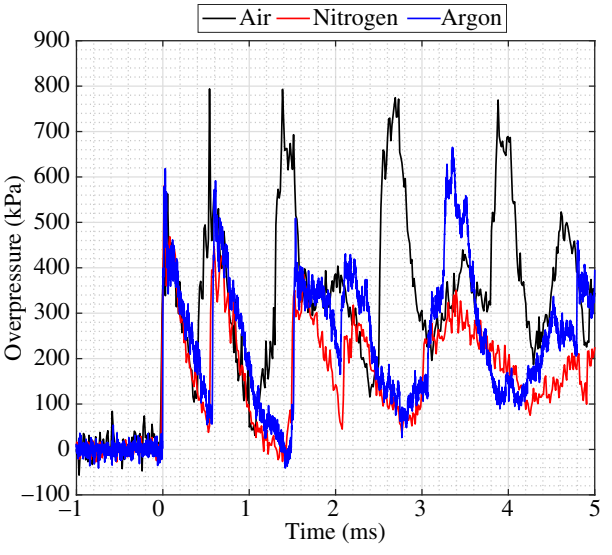

Figure 10. Raw pressure–time history plots for 30 g PE10 spherical detonations within the described confined chamber, with air, nitrogen and argon atmospheres, considering the opening few shock recordings.

atmosphere, despite being in phase with the recordings in nitrogen, exhibits a higher pressure and impulse at each progressive shock recorded. This results in a generally higher long-term QSP when comparing the results of argon and nitrogen, as seen in figure 9. The similar rate of decay in QSP in the long term within all three atmospheres leads to the conclusion that this decay is due to thermal losses to raising the temperature of the chamber walls.

The duration of afterburn reactions can be inferred from the very early-stage pressure–time traces in air and inert atmospheres (figures 9 and 10). In the latter, the TDSA QSP trace reaches a maximum value very quickly after detonation. In the former, there is a similar very rapid rise, followed by a slower increase in QSP over the subsequent 10 ms or so. It would seem that the rapid rise is due to the energy released by the initial detonation, whereas the slower additional rise in air is due to afterburn.

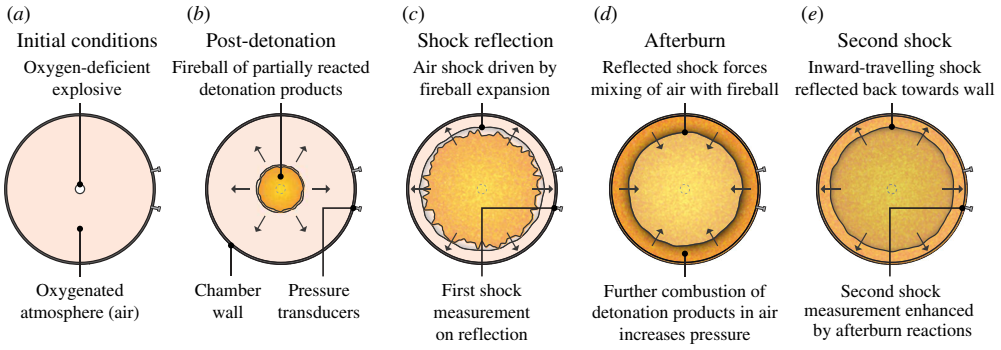

Figure 11. Schematic detailing the phased detonation behaviour of an explosive in a confined chamber highlighting the afterburn mechanism; a) Pre-Detonation Conditions, b) Post-Detonation product expansion, c) Shock interaction on a surface, d) Afterburn as a result of forced combustion, e) Secondary shock enouraging additional afterburn

(d) Compiled experimental results

The previous work published by Farrimond *et al*. [17] characterized PE4, PE8 and PE10 in far-field area-style trials, within which very similar explosive yields were recorded. Presented in this article is an investigation into whether the same explosive compositions behave in a similar manner within a confined scenario. Figure 12 displays the maximum QSP obtained for each explosive composition, detonated within air, nitrogen and argon atmospheres with respect to reduced charge mass, based on the volume of the chamber. The coloured markers relate directly to the results gathered within this article. Conversely, the white markers relate to historical data extracted from the articles presented in table 1.

Clearly seen is a definitive relationship between reduced mass and the maximum QSP extracted, with a distinct consistency between all three plasticized explosive types in air, nitrogen and argon in line with findings suggested within the aforementioned article. The lack of oxygen in nitrogen and argon atmospheres suffocates the combustion process and subsequent fireball development, thus resulting in an inefficient energy release of a given explosive. The difference between argon and nitrogen is solely due to the density of the gas itself and the fundamental difference in wave speeds.

The consistency of these results presents fundamental justification to the deterministic nature of explosive detonation. While some published articles detail large inherent variability in explosive behaviour on yield from nominally identical tests, Rigby *et al*. [16] discussed that at least for far-field free-air scenarios, the parameters could be predicted with a reasonable level of accuracy and suggested explosive events, despite occurring over short durations, can be categorized as deterministic. Confined blasts are far more chaotic, with complex interactions between reflecting shock waves and expanding detonation products. Inferring larger variability ranges within data recorded during these scenarios would not be irrational; however, the fact that there are clear trends in the extracted peak pressure with reduced mass, seen in figures 5 and 12, justifies the deterministic nature of explosive detonation.

5. Numerical modelling

(a) Overview

Published literature data and previous trials conducted by the current authors exhibit low levels of variability of experimentally recorded far-field loading from a given charge composition, shape and mass. The importance of these findings provides a starting point to establish

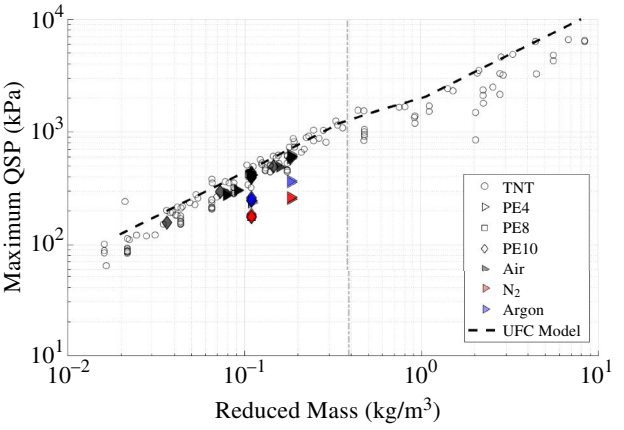

Figure 12. Compiled processed max. QSP data from three different high explosives tested against the mass-to-volume ratio of explosive tested within three different atmospheric volumes and compared with historical TNT data.

characteristics of more challenging blast loading conditions both in the near-field and those in complex environments, knowledge of which can be supplemented with high-fidelity, validated numerical modelling.

Understanding the mechanisms and magnitudes of blast loading on structures from both near-field detonations of high explosive, and those in complex environments, is of key importance for the analysis and design of the response of protective structures. However, there is relatively little definitive experimental data on the measurement of these loads, and consequently, the predictions of numerical models of near-field blast loading are largely unvalidated. The experimental results from this article have been used to validate near-field numerical models for PE4, PE8 and PE10, using the methodology outlined in Whittaker *et al*. [38], which can be implemented into much more complex numerical simulations to produce validated and accurate predictions.

(b) Model description

The models placed each charge on the central axis of the modelled chamber, with the charge centre located 270 mm from one end of the cylinder, as per the experimental methodology, and the charges were centrally detonated. The model used quarter symmetry to improve numerical efficiency by placing reflected boundaries along each surface, with a cylindrical object used to define the geometry of the test chamber (1 m long and 305 mm internal radius). The numerical model was solved using APOLLO blast simulator [39], which makes the use of adaptive mesh refinement (AMR), and zoom levels (distance-dependant AMR) to allow finer mesh resolution to be used within the complex regions of numerical analysis, in close proximity of the detonation and the initial propagation [40,41]. The AMR process requires user-defined zone length, corresponding to the coarsest cell size, and a maximum resolution level size, which corresponds to the smallest allowable cell size. The software then refines and un-refines different zones within the model (based on differentials of pressure, material, etc.) to accurately simulate the event while maximizing efficiency. The model also uses 'zoom levels' which allows a higher resolution level to be used for a fixed radius from the charge centre (e.g. a zoom level of 1 for 200 mm would increase the maximum resolution level by 1 until a disturbance is registered at 200 mm, and the model would then only allow the initial maximum resolution level to be achieved for the remainder of the model). AMR was used for computational efficiency, and explicit afterburn was included for all models simulated within an air environment. The tests conducted with a nitrogen environment were simulated in air with afterburn turned off.

The general resolution used was as follows:

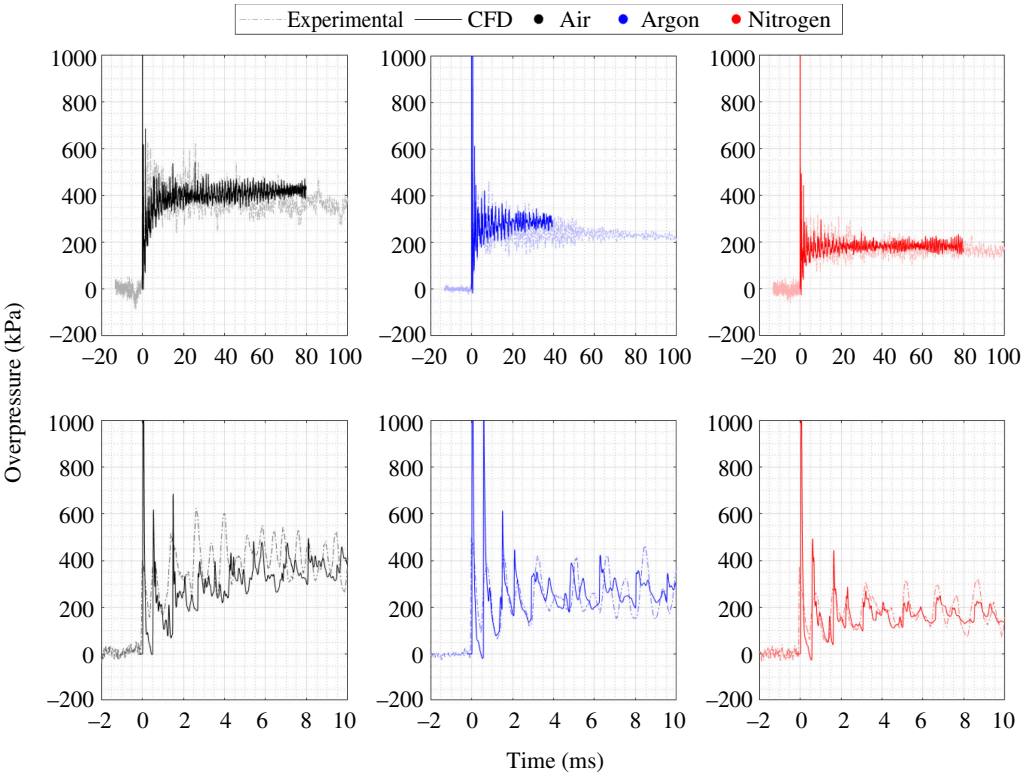

Figure 13. Comparison between experimentally recorded 30 g PE10 charges in air (black), argon (blue) and nitrogen (red) to Apollo numerical modelling.

- *Zoom level 5*. 0.195 mm for 25 mm radius.
- *Zoom level 4*. 0.391 mm for 50 mm radius.
- *Zoom level 3*. 0.781 mm for 100 mm radius.
- *Zoom level 2*. 1.56 mm for 200 mm radius.
- *Zoom level 1*. 3.125 mm for 450 mm radius.
- 6.25 mm used for remainder of model up to 80 ms.

(c) Model results

The modelling results displayed in figure 13 captured the physical behaviour of the confined detonation of 30 g PE10 explosive within each atmosphere. Clear in both the air and nitrogen shots is the general agreement between the computational fluid dynamic (CFD) simulations and experimental data within the opening ~20 ms, after which the experimental data begin to decay. As noted earlier, this decay is believed to be associated with the loss of thermal energy from the chamber atmosphere to the chamber walls, a phenomenon that is not captured within the CFD simulation. This aspect is discounted, and the numerical model results display a remarkable consistency with the experimental data, providing confidence in the use of the numerical modelling approach for practical evaluation of confined detonations of these plasticized high explosives.

Extracted from the CFD simulations was the mass of detonation products with respect to the time after charge initiation, as seen in figure 14. The results when normalized suggest that at ~20 ms, the majority of the afterburn process has occurred and therefore no further release of

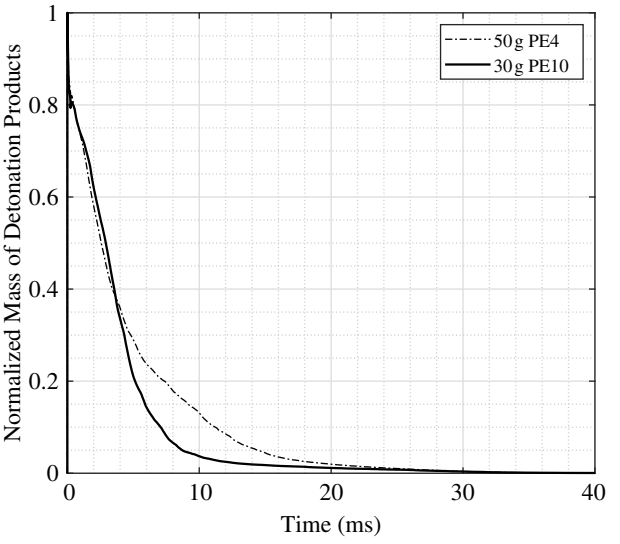

Figure 14. CFD generation of the normalized mass of detonation products with respect to time from the initiation of both 50 g PE4 and 30 g PE10 within an air atmosphere.

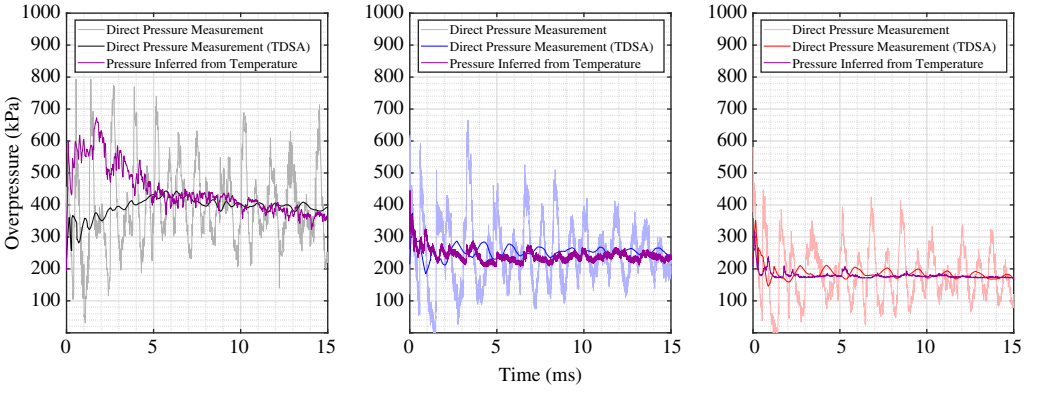

Figure 15. Experimentally recorded pressure–time history resulting from a 30 g PE10 detonation in air (black - left), argon (blue - centre) and nitrogen (red - right) using pressure gauges and inferred pressures from the IRT using the ideal gas laws.

energy occurs. This provides an additional justification as to why thermal conditions within the chamber are able to decay.

6. Inferred pressure from temperature measurements

Published literature has worked on the assumption that confined blasts parameters can be predicted using the ideal gas law theory under which the pressure within a vessel is directly related to the temperature of the gas provided a constant volume [11]. This assumption was investigated in this study by independently recording pressure and temperature in the same event. A bespoke high-speed (250 kHz) infrared radiation thermometer (IRT) was developed that has the ability to measure the temperature of a given medium based on the emitted radiance of a fireball. Hobbs *et al*. [42] provide details on the specification, design, manufacture and calibration of the IRTs used in this study. Using the ideal gas law theory (equation 6.1), the temperature measurements, T, can be used to infer the temporal development of pressure,

P, in a constant volume, V, with the known moles of gas in the chamber, n, and gas constant, R = 8.314 J/(mol K). Each IRT measured the emission of light on two wavelength spectra and provided two individual traces. These have been averaged to provide the best representation of the IRT temperature recordings.

$$PV = nRT\,. \tag{6.1}$$

Figure 15 displays the inferred pressure–time histories from the IRT versus those recorded using the pressure gauges. Across all three environments, it is clear to see that despite the early-time discrepancy between the TDSA and the inferred pressures, believed to be related to flame temperature of the fireball, there is reasonable agreement. These results provide confidence in assuming the ideal gas law theory stands for confined blast loads, validated through two different parameter recording methods.

7. Conclusion

We have presented a study of the pressures generated by the reaction of small charges of plasticized explosive in a confined chamber. The following conclusions have been reached.

- When care is taken with the experimental set-up, the recorded pressure–time relations are highly repeatable. This finding applies not only to the time-averaged trend QSP but also to the temporal variations in the recorded pressure due to the propagation and multiple reflections of shock waves in the chamber.
- Tests conducted in inert atmospheres, where the secondary afterburn of partially reacted detonation products is prevented, resulted in significantly lower QSP. In these inert atmosphere tests, the trend QSP rose rapidly (<<1 ms) to a peak value, whereas the form of the pressure–time trend in the reactive atmosphere tests was a similar sharp rise, followed by a slower (order of milliseconds) climb to peak. It is believed that the initial rise reflects the pressure change due to detonation, with the slower rise being due to the afterburn reaction.
- Numerical modelling of these events conducted using a CFD code that explicitly calculates the temporal development of the afterburn reaction gave pressure–time predictions which compared well with the consistent experimental results.
- Independent measurement of pressure and temperature in the chamber produced data that generally correlated well when compared with using the ideal gas relation. However, there was a discrepancy between the two measurements in the first few milliseconds after detonation in tests conducted in an air atmosphere, with the direct temperature measurements implying significantly more energetic conditions than did the pressure measurements. This feature was significantly less pronounced in the tests in inert atmosphere. As the duration of the discrepancy approximately matches that of the rise in pressure believed to be due to afterburn, it is suggested that the temperature measurement is actually recording the afterburn flame temperature at early times.
- The long-term match between the temperature and pressure measurements indicates that gas venting in the test arrangement was insignificant. However, there was a pronounced monotonic fall in recorded QSP magnitude from the initial peak. This is believed to be due to thermal energy transfer from the hot post-explosion atmosphere, to the steel walls of the chamber. This suggests that the standard model of QSP magnitude versus time being affected only by reduced charge mass and venting of gas to the external environment may be questionable.

This study aimed to establish a benchmark in the consistency of confined blast pressures as a result of detonating various explosive compositions within a confined chamber. Through the utilization of inert atmospheres of nitrogen and argon, the combustion process can be omitted. The results of this are compared directly with trials conducted within air, to evaluate the rate at

which afterburn occurs, and its contribution to the overall QSP. Understanding and quantifying the detonation and subsequent combustion process are significant towards the development of fast-running engineering models that are able to predict blast pressures as a result of internal blasts.

Data accessibility. New data have been provided as supplementary material and existing data referenced accordingly [43].

Declaration of AI use. We have not used AI-assisted technologies in creating this article.

Authors' contributions. D.G.F.: conceptualization, data curation, formal analysis, investigation, methodology, project administration, software, supervision, validation, visualization, writing—original draft, writing—review and editing; S.W.: data curation, formal analysis, investigation, methodology, writing—review and editing; A.D.B.: conceptualization, funding acquisition, investigation, methodology, writing—review and editing; T.L.: data curation, investigation, methodology, project administration, writing—review and editing; A.T.: conceptualization, funding acquisition, investigation, project administration, supervision, writing—review and editing; R.W.: data curation, investigation, methodology, writing—review and editing; S.D.C.: conceptualization, funding acquisition, supervision, writing—review and editing; S.E.R.: conceptualization, funding acquisition, methodology, project administration, supervision, writing—review and editing; M.J.H.: conceptualization, data curation, formal analysis, investigation, resources, software, writing—review and editing; J.R.W.: conceptualization, funding acquisition, investigation, project administration, supervision, writing—review and editing; M.W.: data curation, formal analysis, funding acquisition, investigation, software, validation, writing—review and editing; D.J.P.: conceptualization, funding acquisition, project administration, resources, supervision, writing—review and editing; M.H.: conceptualization, data curation, methodology, writing—review and editing.

All authors gave final approval for publication and agreed to be held accountable for the work performed therein.

Competing interests. We declare that we have no competing interests.

Funding. Experimental work for PE4 and PE10 reported in this article was funded by the Engineering and Physical Sciences Research Council (ESPRC) as part of the Mechanisms and Characterisation of Explosions (MaCE) project, EP/R045240/1. The experimental work consisting of PE8 was funded directly by Dstl. D.F. gratefully acknowledges the financial support from the EPSRC Doctoral Training Partnership and Dstl. A.T. gratefully acknowledges financial support from the Royal Academy of Engineering and Dstl.

Acknowledgements. The authors wish to thank the technical staff at Blastech Ltd. for their assistance in conducting the experimental work.

References

1. Kuhl AL, Forbes J, Chandler J, Oppenheim AK, Spektor R, Ferguson RE. 1998 *Confined combustion of TNT explosion products in Air*. Technical Report-LLNL Report UCRL-JC-131748. Livermore, CA: Lawrence Livermore National Laboratory.
2. Kuhl AL, Oppenhiem AK, Ferguson RE, Reichenback H, Newald P. 2000 Effects of confinement on combstion of TNT explosion products in air. In *28th International Symposium of Combustion, Edinburgh, Scotland*.
3. Ornellas DL. 1989 Calorimetric determination of the heat and products of detonation of an Unusual CHNOFS Explosive. *Propellants. Explo. Pyrotec.* **14**, 122–123. (doi:10.1002/prep.19890140308)
4. Wolanski P, Gut Z, Trzcinski WA, Szymanczyj L, Paszula J. 2000 Visualization of turbulent combustion of TNT detonation products in a steel Vessele. *Shock. Waves.* **10**, 127–136. (doi:10.1007/s001930050186)
5. AndersonCE, Baker WE, Wauters DK, Morris BL. 1983 Quasi-static pressure, duration, and impulse for explosions (e.g. HE) in structures. *Int. J. Mech. Sci.* **25**, 455–464. (doi:10.1016/0020-7403(83)90059-0)
6. Wei Z, Zhou T. 2013 Calculation of quasi-static pressures for confined explosions considering chemical reactions under Isobaric assumption. *Exp. Shock Waves* **S1**, 78–83. (doi:10.4028/www.scientific.net/AMM.164.396)
7. Donahue L, Zhang F, Ripley RC. 2013 Numerical models for afterburning of TNT detonation products in air. *Shock Waves* **23**, 559–573. (doi:10.1007/s00193-013-0467-2)

8. Fried LE. 1994 *Cheetah 1.0 users Manual*. Technical Report-LLNL Report: UCRL-MA-117541. Livermore, CA: Lawrence Livermore National Laboratory.
9. Fried LE. 1994 *Cheetah: A next generation Thermochemical Code*. Technical Report-LLNL Report: UCRL-ID-117240. Livermore, CA: Lawrence Livermore National Laboratory.
10. Trzcinski WA, Paszula J, Wolanski P. 2006 Thermodynamic analysis of Afterburning of detonation products in confined explosions. *J. Energetic. Mater.* **20**, 195–222. (doi:10.1080/07370650208244821)
11. Edri IE, Grisaro HY, Yankelevsky DZ. 2019 TNT equivalency of different explosives in a confined space. In *18th International Symposium on the Effects of Munitions on Structures, Panama City Beach, FL, 21–25 October*. ISIEMS.
12. Edri I, Feldgun VR, Karinski YS, Yankelevsky DZ. 2012 On blast pressure analysis due to a partially confined explosion: III. Afterburning effect. *Int. J. Prot. Struct.* **3**, 311–331. (doi:10.1260/2041-4196.3.3.311)
13. Griffiths H, Pugsley A, Saunders O. 1968 *Report of the inquiry into the collapse of flats at Ronan point, Canning Town: presented to the Minister of Housing and Local Government*. London, UK: HMSO.
14. Baker WE, Hokanson JC, Esparza ED, Sandoval NR. 1983 *Gas pressure loads within vented and Unvented Structures*. Technical Report ADP001739. San Antonio, TX: Southwest Research Institute.
15. Baker WE, Cox PA, Westine PS, Kulesz JJ, Strehlow RA. 1983 *Fundamental studies in engineering 5: explosion hazards and evaluation*. Amsterdam, the Netherlands: Elsevier. See http://deepblue.lib.umich.edu/handle/2027.42/25541.
16. Rigby SE, Tyas A, Fay SD, Clarke SD, Warren JA. 2014 Validation of semi-empirical blast pressure predictions for far field explosions - is there inherent variability in blast wave parameters. In *6th International Conference on Protection of Structures Against Hazards, Tianjin, China*, pp. 1–9. (doi:10.1260/2041-4196.6.1.23)
17. Farrimond DG, Woolford S, Tyas A, Rigby SE, Clarke SD, Barr A, Whittaker M, Pope DJ. 2024 Far-field positive phase blast parameter characterisation of RDX and PETN based explosives. *Int. J. Prot. Struct.* **15**, 141–165. (doi:10.1177/20414196221149752)
18. Edri IE, Savir Z, Feldgun VR, Karinski YS, Yankelevsky DZ. 2011 On blast pressure analysis due to a partially confined explosion: I. experimental studies. *Int. J. Prot. Struct.* **2**, 1–20. (doi:10.1260/2041-4196.2.1.1)
19. Feldgun VR, Karinski YS, Edri IE, Yankelevsky DZ. 2016 Prediction of the quasi-static pressure in confined and partially confined explosions and its application to blast response simulation of flexible structures. *Int. J. Impact Eng.* **90**, 46–60. (doi:10.1016/j.ijimpeng.2015.12.001)
20. Weibull HRW. 1968 Pressures recorded in partially closed chambers at explosion of TNT charges. *Ann. N. Y. Acad. Sci.* **152**, 357–361. (doi:10.1111/j.1749-6632.1968.tb11987.x)
21. US Department of Defence. 2008 *Structures to resist the Effects of accidental Explosions*. UFC 3-340-02. US DoD, Washington, DC.
22. Schwer L, Rigby SE. 2017 Reflected secondary shocks: Some observations using afterburning. In *11th European LS-Dyna Conference.* DynaMore: Salzburg, Austria.
23. Maiz L, Paszula J. 2016 Studies of confined explosions of composite explosives and layered charges. *J. Energetic. Mater.* **14**, 957–977. (doi:10.22211/cejem/65075)
24. Zhang F, Anderson J, Yoshinaka A. 2007 Post-detonation energy release from TNT-aluminium explosives. In *Proceedings of the Conference of the American Physical Society Topical Group on Shock Compression of Condensed Matter*. Waikoloa, Hawaii.
25. Zhou H, Zheng C, Yue X, Zhu Z, Lu A, Kong X, Wu W. 2023 TNT equivalency method in confined space based on steel plate deformation. *Int. J. Impact Eng.* **178**, 104587. (doi:10.1016/j.ijimpeng.2023.104587)
26. Esparza ED, Baker WE, Oldham GA. 1975 *Blast pressures inside and outisde suppressive structures*. Technical Report-Contractor Report EM-CR-76042. San Antonio, TX: Southwest Research Institute.
27. Kong X, Zhou H, Xu J, Zheng C, Lu A, Wu W. 2023 Scaling of confined explosion and structural response. *Thin-Walled Struct.* **186**, 110656. (doi:10.1016/j.tws.2023.110656)

28. Carney KS, DuBois P, Cudziło S, Jorgensen GA, Binienda WK. 2022 The effect of TNT mass and standoff distance on the response of fully clamped circular aluminum plates to confined air-blast loading. *Int. J. Impact Eng.* **170**, 104357. (doi:10.1016/j.ijimpeng.2022.104357)
29. Willauer HD, Ananth R, Farley JP, Williams FW. 2009 Mitigation of TNT and destex explosion effects using water mist. *J. Hazard. Mater.* **165**, 1068–1073. (doi:10.1016/j.jhazmat.2008.10.130)
30. Chen J, Xu C. 2022 Reflected secondary shocks: some observations using afterburning. In *Global Academic Research Institute Proceedings, Oxford, UK, 21 October*, pp. 38–42.
31. Kinney GG, Sewell RG, Graham KJ. 1979 *Peak Overpressures for Intrnal Blast*. Technical Report - NWC TP 6089, China Lake, CA: Naval Weapons Center.
32. Rigby SE, Osborne C, Langdon GS, Cooke SB, Pope DJ. 2021 Spherical equivalence of cylindrical explosives: Effect of charge shape on deflection of blast-loaded plates. *Int. J. Impact Eng.* **155**, 103892. (doi:10.1016/j.ijimpeng.2021.103892)
33. Ruetenik JR, Hobbs P, Smiley F. 1979 *Calculation of multiple burst interactions for siz simultaneous explosions of 120 ton ANFO Charges*. Technical report, Washington, DC: Defence Nuclear Agency.
34. Taylor GI. 1950 The formation of a blast wave by a very intense explosion I. Theoretical discussion. *Proc. R. Soc. Lond. A.* **201**, 159–174. (doi:10.1098/rspa.1950.0049)
35. Balakrishnan K, Genin F, Nance DV, Menon S. 2010 Numerical study of blast characteristics from detonation of homogeneous explosives. *Shock Waves* **20**, 147–162. (doi:10.1007/s00193-009-0236-4)
36. Zhang B, Xiu G, Bai C. 2014 Explosion characteristics of argon/nitrogen diluted natural gas–air mixtures. *Fuel* **124**, 125–132. (doi:10.1016/j.fuel.2014.01.090)
37. Trzciński WA, Cudziło S, Paszula J, Callaway J. 2008 Study of the effect of additive particle size on non-ideal explosive performance. *Propellants Explos. Pyrotec.* **33**, 227–235. (doi:10.1002/prep.200800005)
38. Whittaker MJ, Klomfass A, Softley ID, Pope DJ, Tyas A. 2018 Comparison of numerical analysis with output from precision diagnostics during near-field blast evaluation. In *25th International Symposium on Military Aspects of Blast and Shock (MABS)*, The Hague, the Netherlands, 24–27 September.
39. EMI F. 2018 *Apollo Blastsimulator manual, Version: 2018.2*. Technical report, Freiburg, Germany: Fraunhofer Institute for High-Speed Dynamics.
40. Pannell JJ, Panoutsos G, Cooke SB, Pope DJ, Rigby SE. 2021 Predicting specific impulse distributions for spherical explosives in the extreme near-field using a Gaussian function. *Int. J. Prot. Struct.* **12**, 437–459. (doi:10.1177/2041419621993492)
41. Dennis AA, Pannell JJ, Smyl DJ, Rigby SE. 2021 Prediction of blast loading in an internal environment using artificial neural networks. *Int. J. Prot. Struct.* **12**, 287–314. (doi:10.1177/2041419620970570)
42. Hobbs MJ, Barr AD, Woolford S, Farrimond DG, Clarke SD, Tyas A, Willmott JR. 2022 High-speed infrared radiation thermometer for the investigation of early stage explosive development and fireball expansion. *Sensors* **22**, 6143. (doi:10.3390/s22166143)
43. Farrimond DG *et al.* 2024 Data from: experimental studies of confined plasticised high explosive detonations in inert and reactive atmospheres. The Royal Society. Collection. Figshare. (doi:10.6084/m9.figshare.c.7351601.v1)